諸外国における大気腐食試験の現状について

金属材料技術研究所
福島敏郎

S. C. Britton (The Tin Research Institute) によると，大気腐食に関する実地および促進試験についての組織的活動は今世紀の初期に既に行われていたようである。1908年、ASTMの腐食委員会では5種の低合金鋼を用いて酸浸せきおよび大気暴露による重量減を測定した。1916年、ASTMにおいて鉄鋼の大規模な大気暴露試験が開始され、1920年、Institution of Civil Engineers (英) において海水中における構造材料の劣化に関して世界的規模の試験計画が開始され、同年、大気腐食委員会が Institute of Metals に設立され、次年度からのプロジェクトは BNFMRA に移管された。1931年、ASTMにおいて鉄鋼および非鉄金属材料の20年大気暴露試験が各地区で開始された。ひるがえって、米国の私企業2社のうち1社が1929年に大気暴露試験を事業として創立され、現在盛況であることは注目に値しよう。

今後進展する大気腐食の分野に屋内腐食 indoor corrosion の問題がある。すなわち、電気・電子機器用の材料・部品に対する使用環境の影響が重大な関心を呼んでおり、長期プロジェクトが国際的規模において展開されようとしている。これらの研究はメーカーとユーザーの両方に役立つデータの集大成を目指すとともに、腐食機構を明らかにすることにより促進試験法の策定と防食設計の確立を目的としている。この分野では Siemens, IBM, Bell Lab, その他の有力な研究所における基礎・応用研究は世界的にトップレベルにあるということができよう。

以下、米国をはじめ各国における研究状勢を紹介するが、これらの諸国は大気腐食の研究キャリアーに富み、その水準が高いとみなすことができる。このほか、インド、チェコスロバキアでも研究が盛んであり、corrosion map などの有益な結果が報告されている。

USSR
Y.N.Mikhailovski,
P.V.Strekalov
Inst.Physical Chemistry,
Academy of Science of
the USSR,Moscow

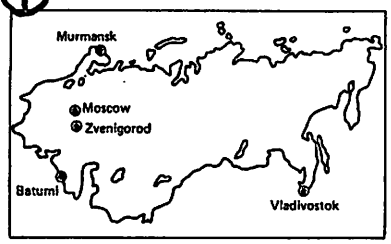

Figure 63.1. IFCHAN atmospheric corrosion test stations.

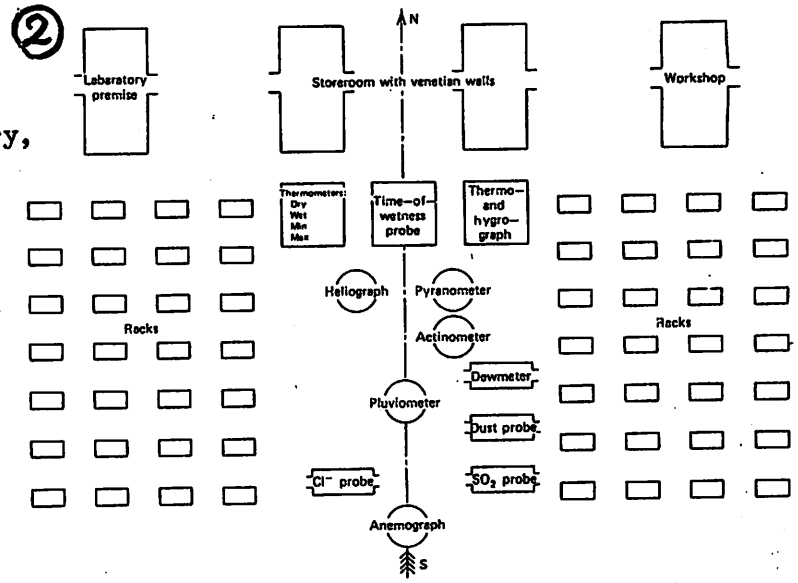

Figure 63.2. Layout of facilities on the testing ground.

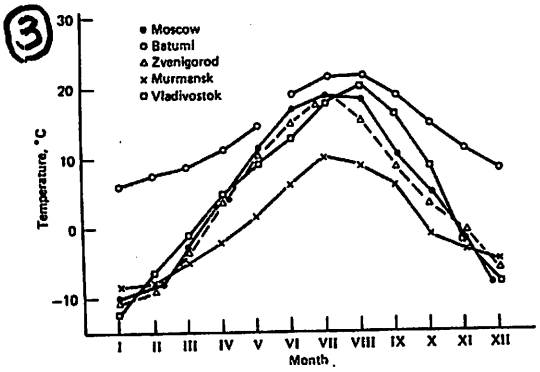

Figure 63.7. Yearly air temperature variations at the test stations.

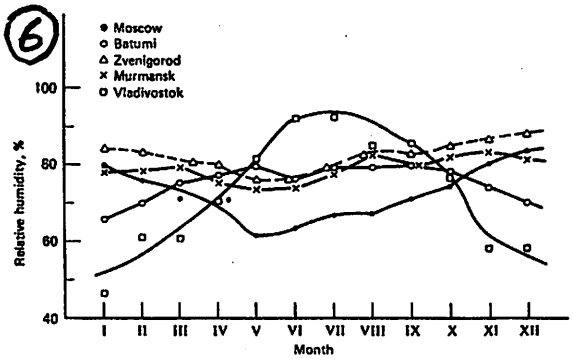

Figure 63.8. Yearly air relative humidity variations at the stations.

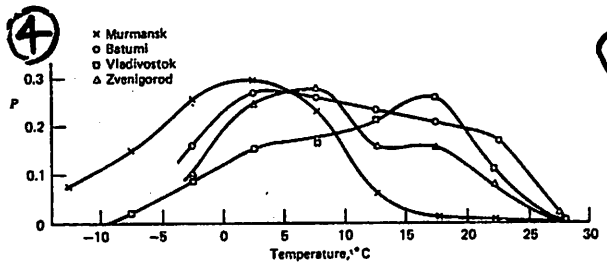

Figure 63.9. Recurrence of air relative humidity over 70% at various temperatures.

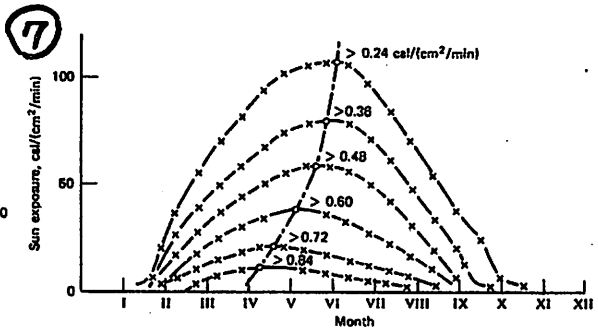

Figure 63.11. Distribution of total solar radiation intensity in a rural environment.

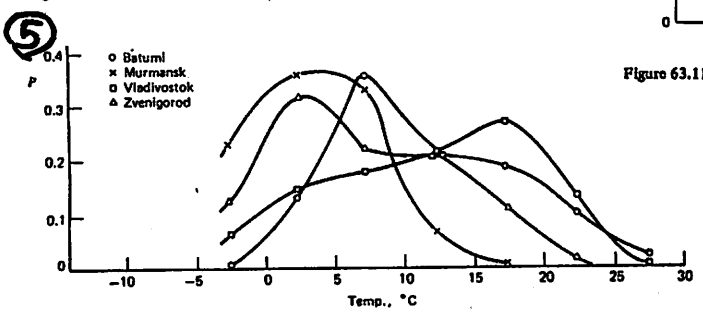

Figure 63.10. Recurrence of water phase films on metals.

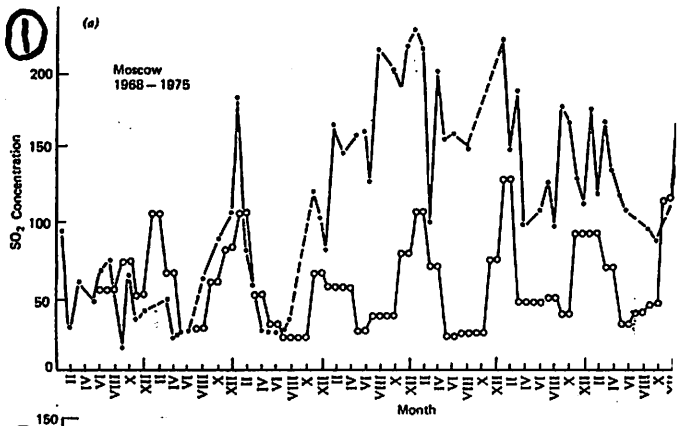

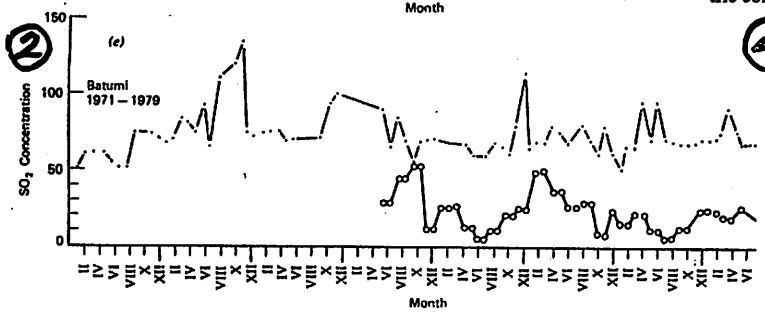

Figure 63.12. SO_2 concentration in the air. –·–·–: Aspiration method (mg/m^3). o–o: Filtrasit method (mg/m^2/day).

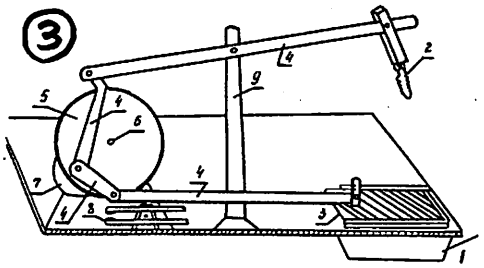

Figure 63.5. Apparatus for sampling and burning sulfur weight amounts. 1–sulfur melt bath with thermostat, 2–nickel-chrome heater, 3–bath lid, 4–system of levers, 5–disc, 6–electric motor shaft, 7–cam, 8–electric contacts, 9–support.

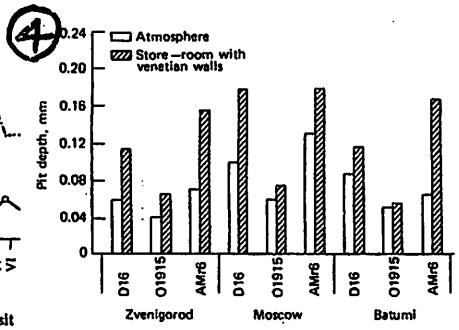

Figure 63.19. Pitting corrosion of aluminum alloys.

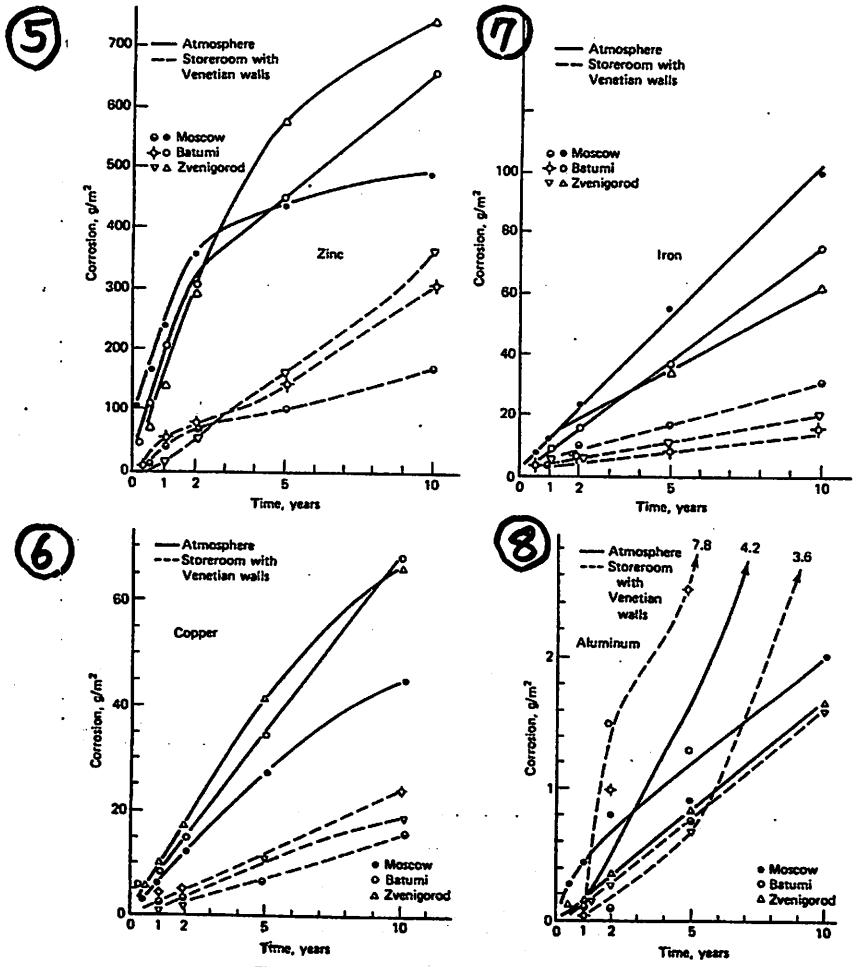

Figure 63.17. Corrosion of steel, copper, zinc, and aluminum.

Tropical China

T. Biestek, Inst. Precision Mechanics,
Warsaw, Poland

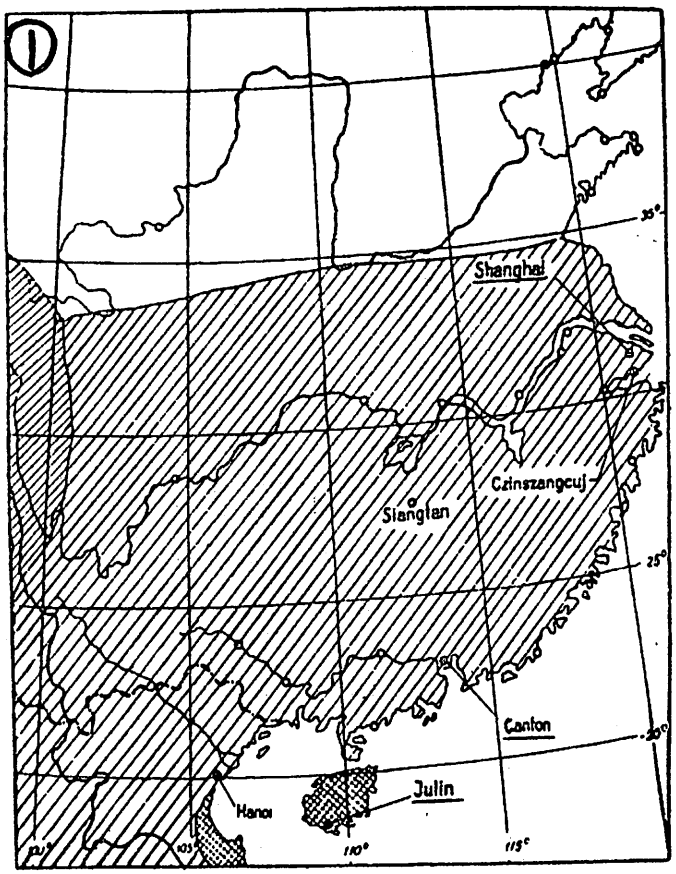

Figure 54.1. The location of exposure sites in China: 1–Tropical and subtropical atmosphere. 2–Tropical humid atmosphere. 3–Tropical dry atmosphere.

③

	Basic metal: St – steel, Cu – copper	Type of coating (see table 2)	Exposure site – Shanghai S10 (open air) Duration of testing (months) 6	12	24	45
1	St	Zn15				
2	St	Zn30				
3	St	Cd6				
4	St	Cd12				
5	St	Cd24				
6	St	Zn15e				
7	St	Cd15e				
8	St	Saf6				
9	St	N124				
10	St	N136				
11	St	Cu8N17Cr1				
12	St	Cu20N110Cr1				
13	St	Cu30N110Cr1				
14	Cu	Cu/Sn24				
15	Cu	Cu/Sn36				
16	Cu	Cu/Ag12				
17	Cu	Cu/Ag24				
18	Cu	Cu/N112Cr1				
19	Cu	Cu/N124Cr1				
20	Cu	Cu/Sn12				
21	Cu	Cu/Sn24				
22	Cu	Cu/Ag12pe				
23	Cu	Cu/Ag12p2				

④

Exposure site – Julin
H2 (open air)
Duration of testing (months)
6 | 12 | 24

②

	Basic metal: St – steel	Type of coating (see table 1)	Exposure site – Canton University K4 (matting shed) Duration of testing (months) 6	12	24	45	58	Exposure site – Canton University K5 (matting shed) Duration of testing (months) 6	12	24	≈5	58
1	St	Zn15										
2	St	Zn30										
3	St	Cd6										
4	St	Cd12										
5	St	Cd24										
6	St	Zn15e										
7	St	Cd15e										
8	St	Zn15cL										
9	St	Cd15cL										
10	St	N127										
11	St	N18										
12	St	N127										
13	St	Cu20N110Cr1										

なし ごく軽微 1% 1~5% 5~10% 10~50% 50~100% 落下

1 2 3 4 5 6 7 8

Figure 54.2. The results of corrosion testing of electrodeposited coatings

Southern Africa
B.G.Callaghan
National Bldg.Research
Inst.,CSIR,Pretoria,
South Africa

TABLE 61.4 CHARACTERISTICS OF THE EXPOSURE SITES–SOUTH AFRICA

Town/city and province		Site	Environment	Industrial pollution
Pretoria, Transvaal	G	CSIR	Rural	Very Low
		Mamelodi	Rural/mild industrial	Low
	E	ISCOR	Industrial	High
Cape Town, Cape Province	D	Ysterplaat	Mild marine	Low
		Docks	Marine	Moderate
	H	Simonstown	Marine	Very Low
Durban, Natal	C	Salisbury Island	Marine	Moderate
	B	Bluff	Severe marine	Moderate/low
Walvis Bay, Cape Province	A	Military Camp	Severe marine	Low
		Rooikop	Desert	Nil
Sasolburg Orange Free State	F	Industrial Site	Industrial	High

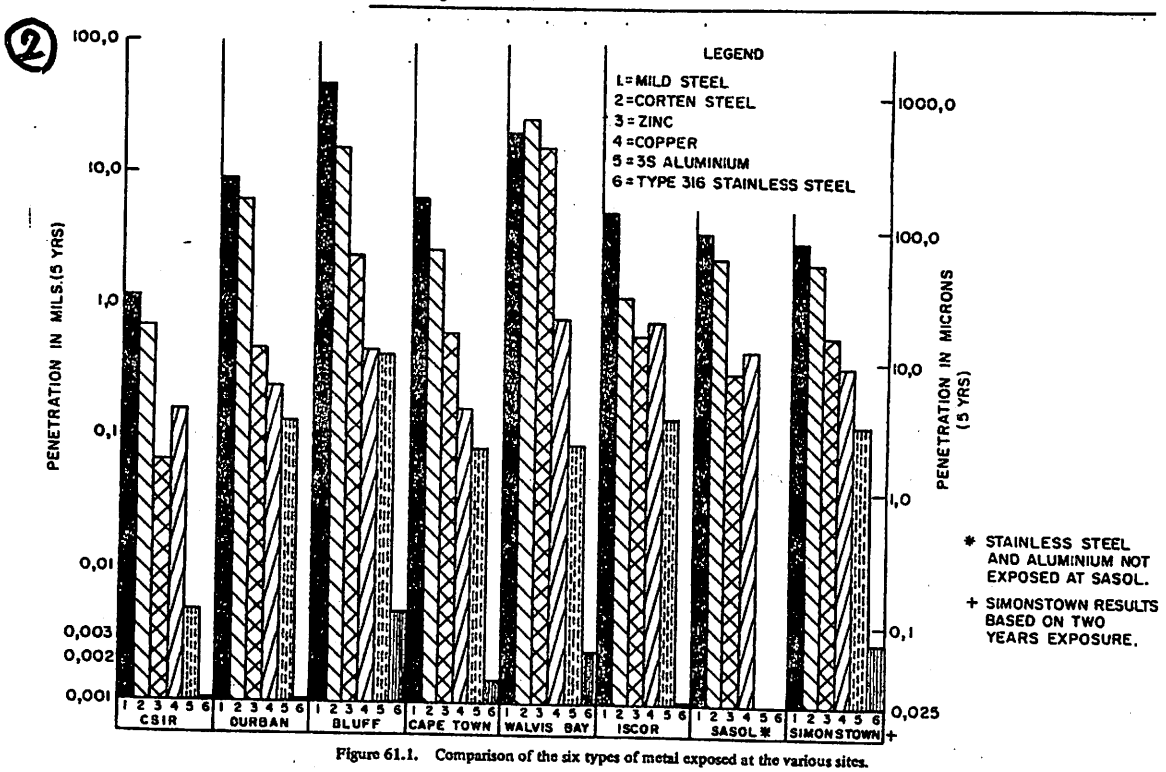

Figure 61.1. Comparison of the six types of metal exposed at the various sites.

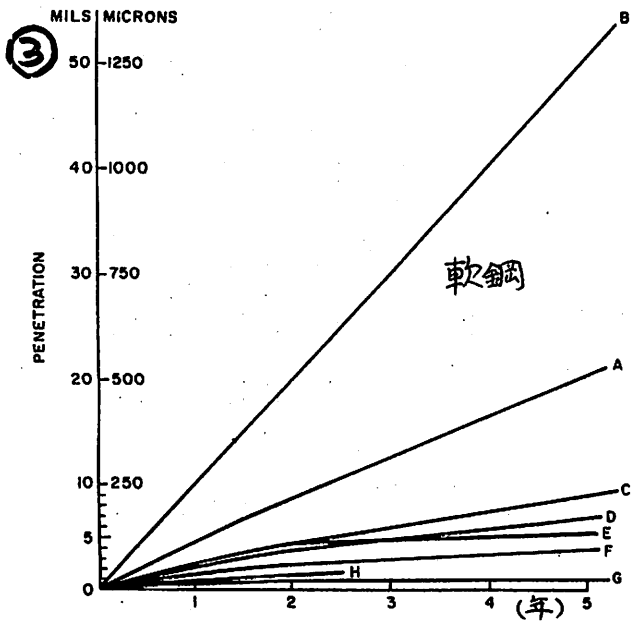

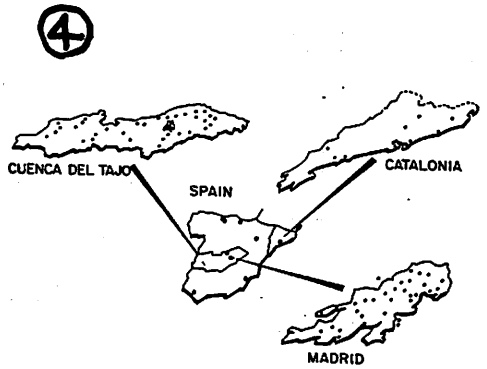

Figure 62.1. Networks of test sites in Spain.

①

南ア

TABLE 61.2 CORROSION RATES AND MAXIMUM PIT DEPTHS OF SHEET ALLOYS, ADDINGTON HOSPITAL, DURBAN

Alcan alloy or metal	Alloy type	Thickness (mm)	Corrosion rate (μ/yr)				Maximum pit depth (mm)			
			2 Years	5 Years	10 Years	20 Years	2 Years	5 Years	10 Years	20 Years
2S-H6	99.2% Al	1.6	1.22	0.97	0.64	0.63	0.17	0.24	0.19	0.13
3S-H4	Al-Mn	1.6	1.22	0.91	0.73	0.76	0.12	0.10	0.19	0.21
65S-TF	Al-Mg-Si	1.6	1.52	1.24	0.89	0.81	0.09	0.07	0.10	0.14
B51S-TF	Al-Mg-Si	1.5	1.22	0.94	0.84	–	0.16	0.21	0.17	–
57S-H6	Al-2.2 Mg	1.6	0.86	0.81	0.61	0.53	0.19	0.24	0.16	0.20
M57S-H6	Al-2.2 Mg	1.6	0.97	0.81	0.79	–	0.18	0.16	0.17	–
C54S-M	Al-3.5 Mg	1.6	0.89	0.79	0.79	–	0.16	0.23	0.23	–
B54S-M	Al-4	1.3	1.12	0.84	0.79	–	0.20	0.34	0.21	–
24S-TB Alclad[a]	99.5 Cladding	1.8	1.22	0.81	0.76	0.63	[b]	[b]	[b]	0.08
75S TF Alclad[a]	72S Cladding	1.6	1.40	1.04	0.79	0.51	[b]	[b]	[b]	0.08
M75S TF Alclad[a]	72S Cladding	1.6	0.97	0.81	0.78	–	0.09	0.09	0.17	–
Zinc		2.3	4.95	4.72	5.21	–				
Lead		1.8	4.14	3.89	–	–				
Copper		0.8	2.06	1.55	1.14	–				
Monel		1.3	1.96	1.63	1.42	1.52				
302 St. Steel		1.3	0.05	0.05	0.03	0.03				

[a] 0.09-mm cladding layer per side. After Godard and Ferguson [11].
[b] All less than 0.08 mm.

TABLE 61.3 CORROSION RATE AND MAXIMUM DEPTH OF PENETRATION FOR ALUMINUM EXTRUSION ALLOYS, ADDINGTON HOSPITAL, DURBAN

Alcan alloy	Alloy type	Corrosion rate (μ/yr)[a]					Max. penetration (mm)				
		2 Years	5 Years	10 Years	15 Years	20 Years	2 Years	5 Years	10 Years	15 Years	20 Years
50S-TE	Al-Mg-Si	4.24	3.05	1.90	1.52	1.02	0.08	0.08	0.18	0.10	0.15
Anodized 50S TE		[b]	[b]	[b]	[b]	[b]	0.41	0.41	1.02	0.89	0.97
24S-TE	Al-Cu-Mg	9.52	8.08	4.55	5.28	[c]	0.15	0.15	2.79	2.41	5.0[c]
26S-TF	Al-Cu	11.18	10.77	7.37	6.22	[c]	0.15	0.10	0.28	0.30	5.0[c]
75S-TF	Al-Zn-Mg-Cu	9.50	13.44	17.14	15.49	15.24	0.05	0.10	0.08	0.46	0.48
A56S-M	Al-Mg	1.07	1.07	0.96	–	–	0.15	0.23	0.28	–	–

[a] After Godard and Ferguson [11].
[b] No mass losses taken.
[c] Areas on samples exfoliated to the extent that no sound metal remains, mass losses thus inaccurate while penetration is greater than 5 mm.

スペイン S. Feliu, M. Morcillo, Centro Nacional de Investigaciones Metalúrgicas, Ciudad Universitaria, Madrid-3, Spain

②

TABLE 62.2 DURATION OF RELATIVE HUMIDITIES OF 85% OR MORE AND TEMPERATURES GREATER THAN 0°C, AVERAGE LEVELS OF POLLUTION WITH SO_2 AND CHLORIDES, AND ANNUAL CORROSION DATA AT VARIOUS TESTING STATIONS THROUGHOUT SPAIN (NUMBERS IN PARENTHESES INDICATE ESTIMATED CORROSION VALUES)

Testing station and annual exposure period	Time at RH > 85% and T > 0°C (in thousands of h/yr)	SO_2 (mg SO_3/dm^2/day)	Chlorides (mg NaCl/dm^2/day)	Corrosion during a one-year exposure					
				Mild steel (μm)		Zinc (μm)		Copper (μm)		Aluminum (mg/dm^2)	
Alicante, 30 m from sea									
(1974–75)	6.8	0.87	0.97	84.0	(81.6)	4.2	(4.8)	3.2	(4.0)	106.3	(110.2)
(1976–77)	4.3	1.57	3.59	92.6	(109.9)	5.8	(7.8)	4.1	(6.4)	73.6	(143.2)
(1978–79)	4.3[a]	1.55	1.66	60.3	(98.6)	6.3	(6.9)	10.0	(6.4)	100.1	(140.9)
Alicante, 100 m from sea									
(1976–77)	4.3	0.16	0.78	26.9	(31.6)	0.93	(3.2)	1.7	(3.2)	14.6	(23.5)
(1978–79)	4.3[a]	0.21	0.25	25.5	(22.6)	1.6	(1.1)	2.4	(1.5)	23.1	(27.4)
Avilés									
(1974–75)	3.7	0.48	[b]	52.0	(37.2)	2.9	(1.9)	3.4	(2.2)	19.8	(12.2)
(1976–77)	3.7[a]	0.48[a]	[b]	42.2	(37.2)	1.5	(1.9)	3.2	(2.2)	9.8	(12.2)
Cabo Negro									
(1974–75)	5.4	0.30	3.77	172.9	(99.2)	12.1	(6.0)	8.1	(4.4)	109.8	(70.0)
(1976–77)	5.0	0.30[a]	1.18	50.9	(75.6)	9.2	(4.9)	5.3	(4.4)	98.8	(66.0)
Barcelona									
(1974–75)	3.2[a]	0.68	0.45[a]	52.2	(43.3)	4.2	(2.3)	3.6	(2.2)	95.4	(70.2)
(1976–77)	3.2	0.65	0.45[a]	49.9	(42.3)	2.2	(2.3)	2.9	(2.2)	41.0	(67.5)
(1978–79)	3.2[a]	0.86	0.45[a]	39.0	(46.4)	2.9	(2.5)	6.7	(2.5)	54.3	(82.1)
Bilbao									
(1974–75)	4.2	1.49	1.40	108.4	(88.5)	7.6	(6.8)	5.8	(6.2)	165.2	(136.5)
(1976–77)	3.0	1.01	0.67	69.6	(67.8)	5.2	(3.8)	4.3	(3.3)	73.8	(83.5)
(1978–79)	3.0[a]	1.01[a]	0.67[a]	75.8	(67.8)	5.6	(3.8)	3.9	(3.3)	85.4	(83.5)
Cádiz									
(1974–75)	4.1[a]	0.31	0.48[a]	43.8	(30.0)	2.3	(2.1)	3.1	(2.5)	93.4	(51.6)
(1976–77)	4.1[a]	0.57	0.48[a]	39.2	(30.7)	1.6	(2.1)	2.4	(2.5)	48.4	(56.4)
(1978–79)	4.1[a]	0.47	0.48[a]	39.9	(30.4)	2.0	(2.1)	1.8	(2.5)	64.3	(55.1)
El Escorial									
(1974–75)	3.9	0.10	[b]	11.3	(8.2)	0.60	(1.1)	1.1	(1.4)	1.5	(1.9)
(1976–77)	3.9[a]	0.10	[b]	7.5	(8.2)	0.87	(1.1)	1.0	(1.4)	1.2	(1.9)
(1978–79)	3.9[a]	0.15	[b]	11.0	(8.2)	2.6	(1.1)	1.0	(1.4)	14.8	(3.7)
Madrid									
(1974–75)	2.1	0.65	[b]	48.4	(30.6)	1.3	(0.89)	1.1	(0.91)	4.8	(7.9)
(1976–77)	2.1[a]	0.70	[b]	43.7	(31.0)	1.4	(0.92)	1.4	(0.94)	2.5	(8.4)
Zaragoza									
(1974–75)	2.1	0.57[a]	[b]	59.0	(30.3)	2.1	(0.82)	1.5	(0.71)	9.6	(7.6)
(1976–77)	2.1[a]	0.57[a]	[b]	31.9	(30.3)	1.1	(0.82)	1.1	(0.71)	1.7	(7.6)

[a] Approximate value.
[b] Negligible value.

Brazil

A.C.Dutra, R.de O.Vianna
Corrosion Consultant, Rio de Janeiro, Brazil
Centro de Pesquisas e Desenvolvimento-Petrobras/ Cenpes, Rio de Janeiro, Brazil

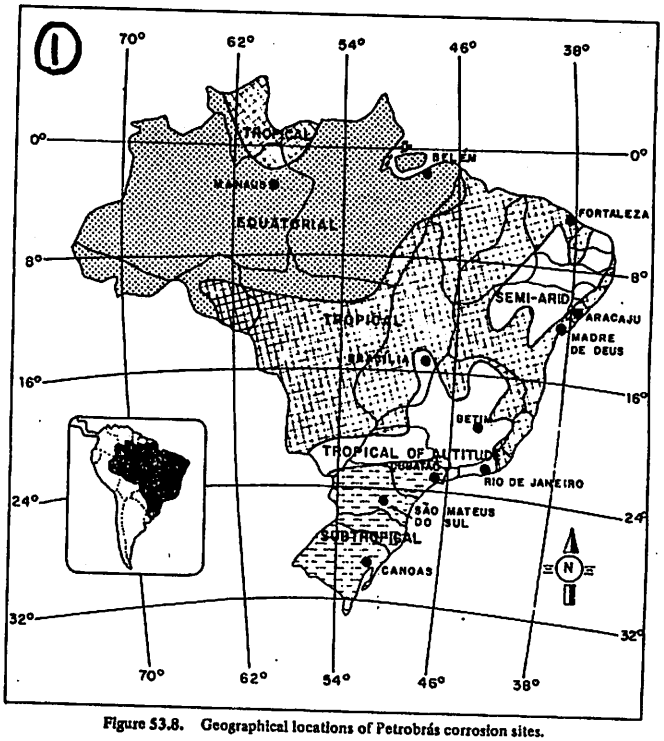

Figure 53.8. Geographical locations of Petrobrás corrosion sites.

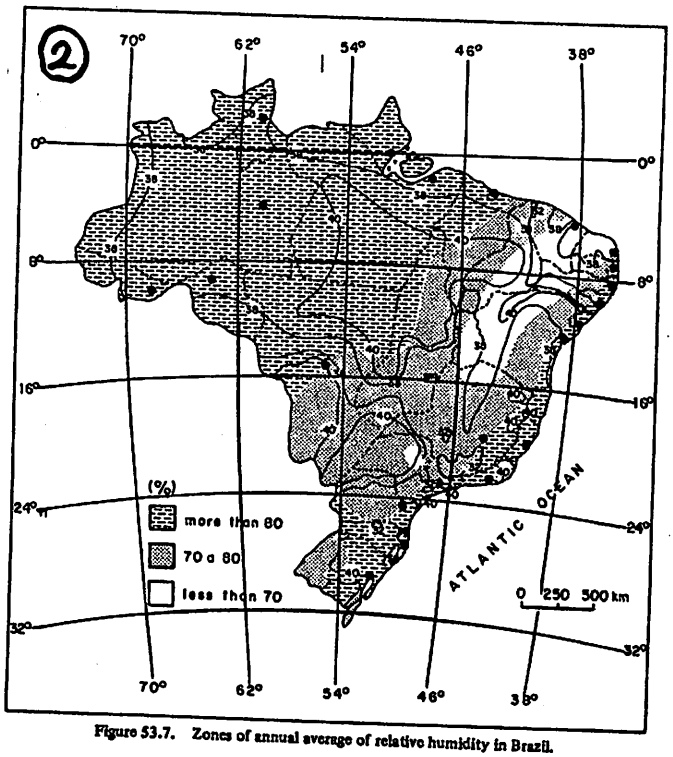

Figure 53.7. Zones of annual average of relative humidity in Brazil.

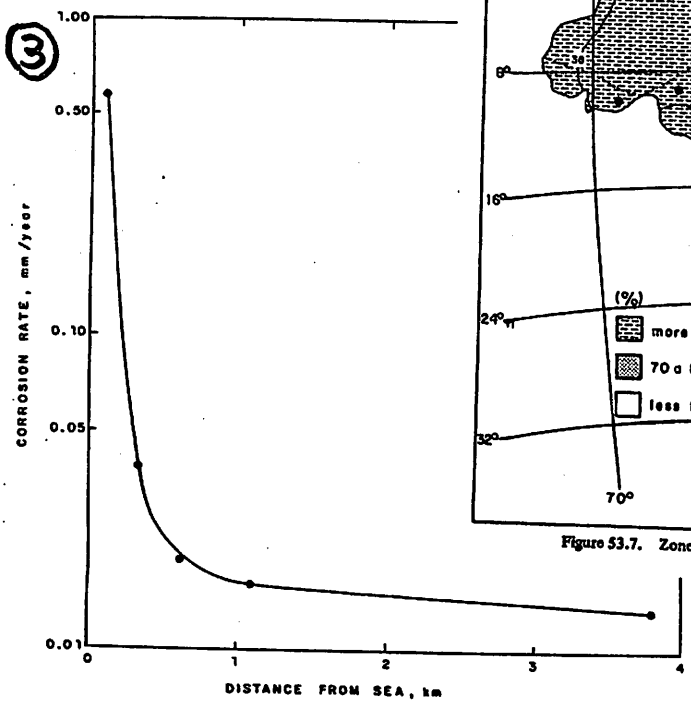

Figure 53.16. Influence of distance from the sea on corrosion rate of carbon steel.

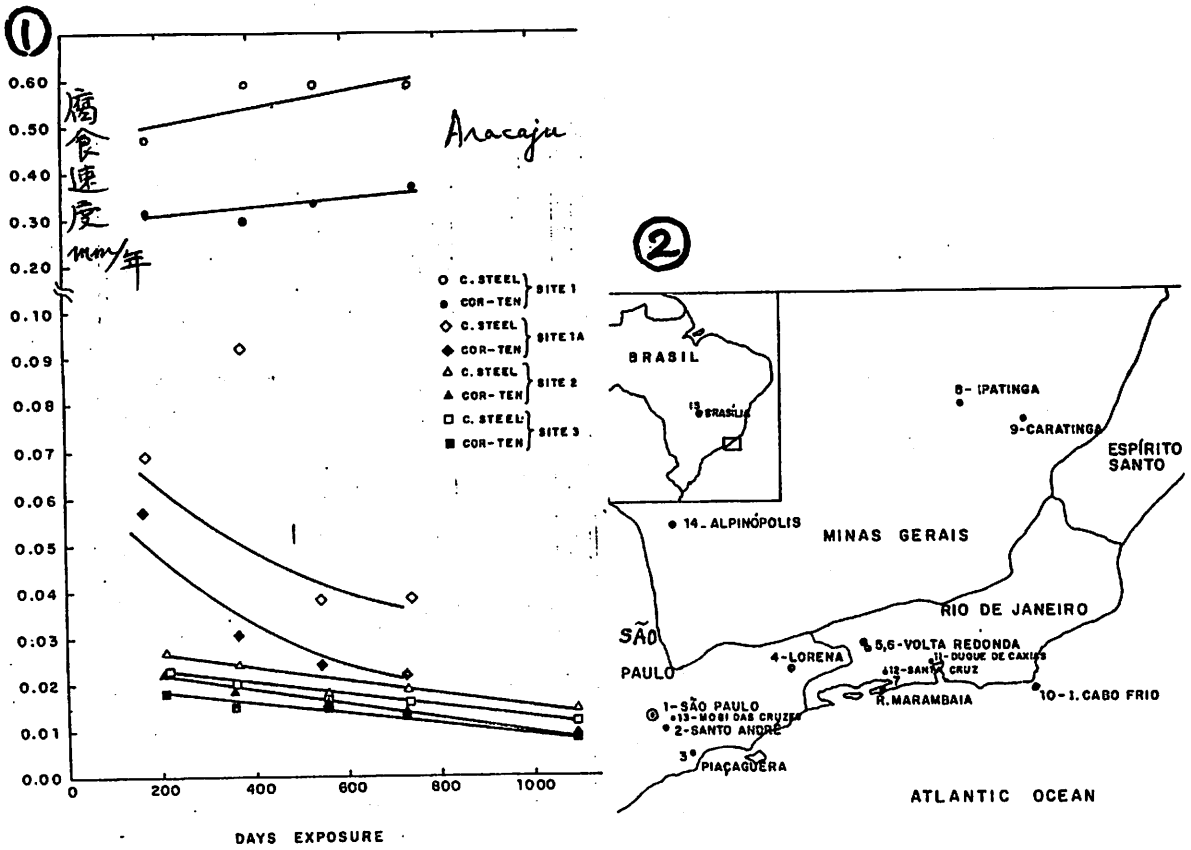

Figure 53.3. Geographical locations of IPT, CEPEL, CSN, and USIMINAS corrosion sites: 3, 4–IPT sites. 5, 6, 7–CSN sites. 8, 9, 10–USIMINAS sites. 11, 12, 13, 14, 15–CEPEL sites. 1, 2,

Australasia

J.F.Moresby, CSIRO Inst. Earth Resources, Div. Mineral Chem., Port Melbourne
F.M.Reeves, Commonwealth Government Paint Committee, Melbourne; D.J.Spedding Dept. Chemistry, The University of Auckland, New Zealand

Figure 52.1. Australasia, showing places mentioned in the text and locations of Atmospheric Corrosion Test Sites, past and present.

② TABLE 52.1 COMPARISON OF CORROSIVENESS OF JTTRE SITES BASED ON STEEL AND ZINC, ONE-YEAR TESTS; EXPOSED VERTICALLY

Locality	Type of atmosphere and contamination	Distance from sea (km)	Corrosion rate (μm) Steel	Zinc
Cloncurry	Hot, dry	600	3.9	0.4
Innisfail	Hot, wet, open, ash from burnt sugar cane	10	23	1.7
Innisfail	Hot wet, under jungle canopy	10	15	1.4
Cowley	Hot wet, coastal sea salt	0.03	129	2.7

Italy

F.Gatto, Istituto Sperimentale dei Metalli Leggeri, Novara, Italy

A.Perrone, Alluminio Journal, Milan, Italy

① TABLE 58.2 CLIMATE DATA OF THE CITY OF MILAN

Month	Average temperature (°C)	Total rainfall (mm)	Average humidity (%)	Average cloudiness (in tenths)	Sky conditions (days)				
					Fog	Rain	Snow	Hoar frost	Storm
January	2.35	197.0	78.11	7.7	1	14	7	7	–
February	6.05	94.6	72.20	7.2	–	10	–	–	–
March	10.70	138.4	63.65	6.0	3	9	–	–	–
April	12.81	56.6	49.72	5.7	–	10	–	–	–
May	15.76	156.2	60.59	6.3	–	16	–	–	–
June	20.56	61.2	50.57	5.9	–	13	–	–	–
July	23.80	190.2	65.66	4.6	–	12	–	–	8
August	22.55	193.2	71.15	5.9	–	15	–	–	9
September	19.03	26.4	68.76	3.6	–	3	–	–	1
October	15.35	111.0	82.25	6.4	5	9	–	–	1
November	8.63	16.4	71.20	5.7	4	6	1	1	–
December	3.76	35.8	70.57	4.6	5	4	1	10	–
1977 Average	13.44	127.7	67.04	–	18	121	9	18	28

② 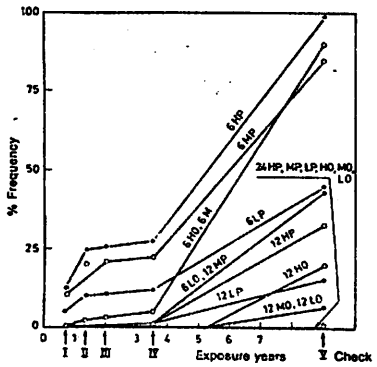

Figure 58.16. Pattern of pitting in marine atmosphere versus years of exposure. Corrosion degree is determined by the ISO 1462/72 method, consisting in laying on the surface a template net with squares 5 mm on a side and in establishing the percentage of squares containing one or more corrosion pits.

③ 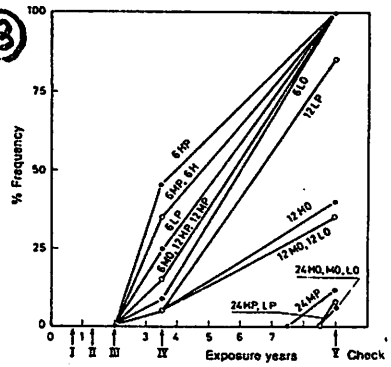

Figure 58.17. Pattern of pitting in urban-industrial atmosphere for L = low Fe; M = medium Fe; H = high Fe; 0 = extruded from direct chill castings; P = extruded from mold castings.

④ TABLE 58.4 PARTICLE SIZE OF Fe-BEARING COMPOUNDS AND THEIR AVERAGE NUMBER PER CM³

Material	Fe (%)	Intermetallic compounds				
		Type A 6 + 15 μm	Type B 4 + 6 μm	Type C 2 + 4 μm	Type D 2 μm	A + B + C + D
HP	0.43	15,000	30,000	60,000	180,000	285,000
MP	0.17	13,000	20,000	30,000	50,000	113,000
LP	0.08	–	10,000	40,000	50,000	100,000
HO	0.43	–	18,000	60,000	250,000	328,000
MO	0.17	–	8,000	20,000	200,000	228,000
LO	0.08	–	–	10,000	160,000	170,000

⑤ 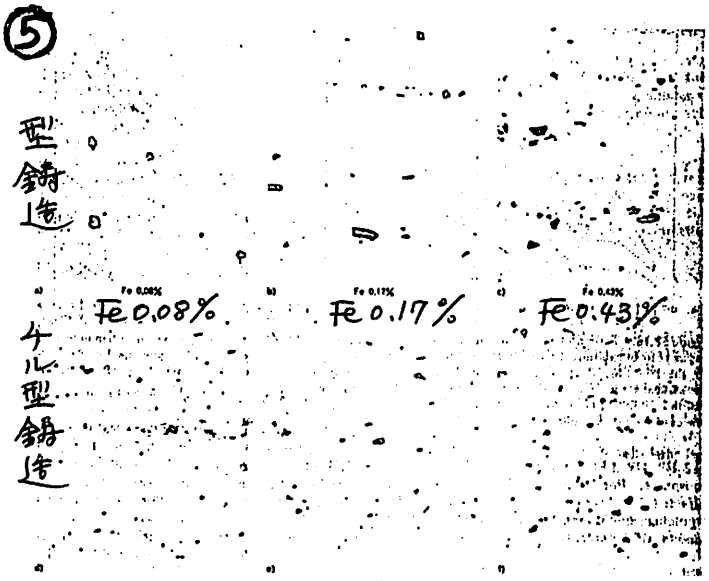

Figure 58.15. Typical structures of intermetallic iron compounds observed on the surface of extruded samples. Above: from mold castings; below: from direct chill castings. From left to right: iron contents 0.08%, 0.17%, 0.43%.

⑥ 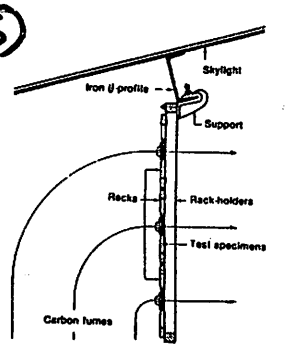

Figure 58.3 Installation of test specimen holders on the skylight of Milan's railroad station.

Type A. 2 X 4 X 6 μm to 4 X 4 X 15 μm bits

Type B. Smaller crystals, generally having a more round shape, with 4 to 6 μm average diameter

Type C. Even smaller crystals of the same kind, with 2 to 4 μm average diameter

Type D. Very fine crystals, with diameter less than 2 μm

Federal Republic of Germany

G.Oelsner, Bundesanstalt für Materialprüfung (BAM), Berlin

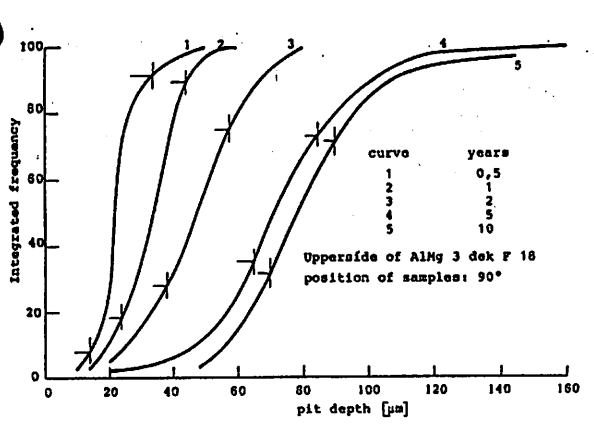

Figure 56.10. Integrated frequency of pit depths as a function of exposure time.

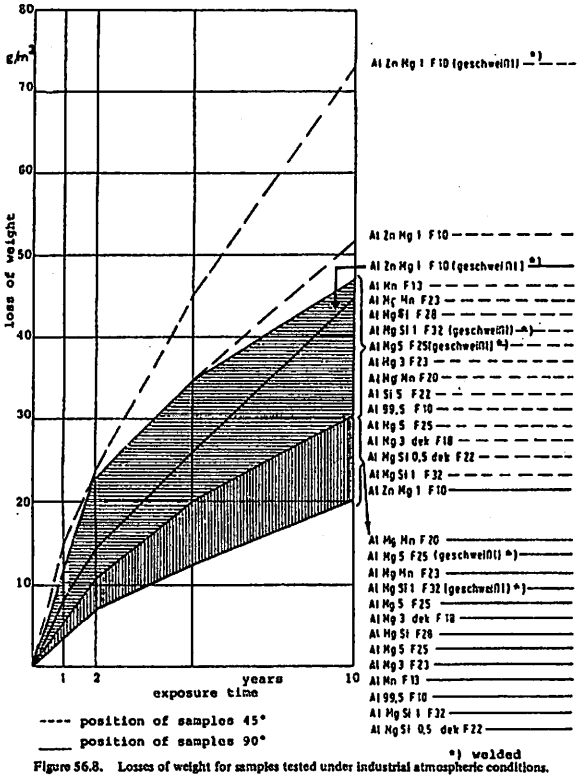

Figure 56.8. Losses of weight for samples tested under industrial atmospheric conditions.

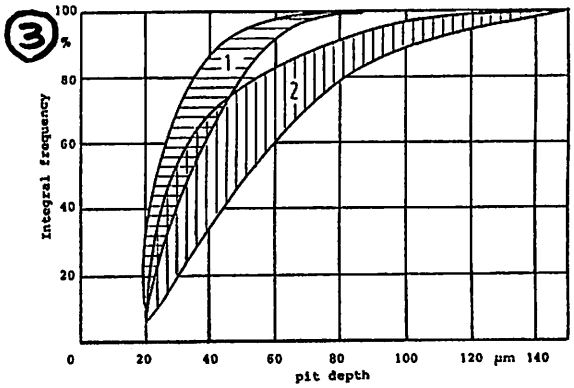

1: Al 99,5 F 10 upper- and underside
AlMn F 13 upper- and underside
AlMg 3 F 23 upper- and underside
AlMgMn F 23 upper- and underside
AlMgSi F 28 upper- and underside
AlMg 5 F 25 upper- and underside
AlMgSi 1 (welded) upper- and underside
AlZnMg1 (welded) upper- and underside
AlMgSi 0,5 dek F 22 upperside
AlMgSi 1 F 32 upperside
AlSi 5 F 22 upperside

2: AlMg 3 dek F 18 upper- and underside
AlMgMn F 20 upper- and underside
AlMg 5 (welded) upper- and underside
AlZnMg 1 F 36 upper- and underside
AlMgSi 0,5 dek F 22 underside
AlMgSi 1 F 32 underside
AlSi 5 F 22 underside

Figure 56.11. Integrated frequency of pit depths after an exposure time of 10 years (coast region; position of samples 45 degrees).

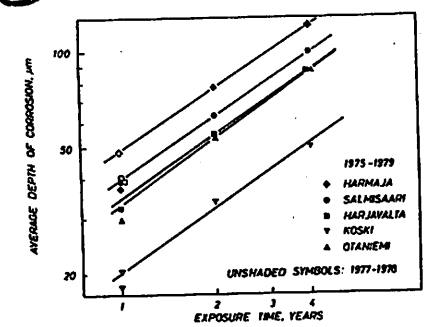

Figure 55.1. Corrosion of mild steel as a function of exposure time from a four-year test series (1975–1979) and a one-year test (1977–1978) on the same steel.

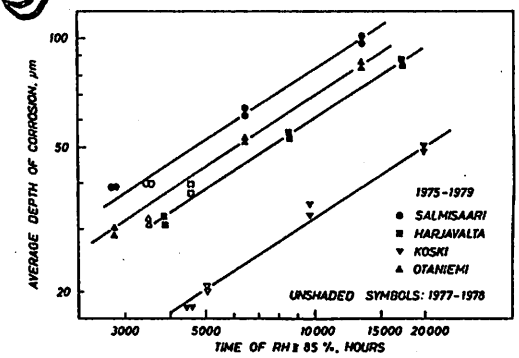

Figure 55.2. Corrosion of mild steel as a function of the time-of-wetness (RH ≧ 85%). Results from a four-year test series (1975–1979) and a one-year test (1977–1978) on the same steel.

Finland

T.Hakkarainen, Technical Research Center of Finland(VTT)
S.Yläsaari
Helsinki University of Technology(TKK)
Dept.Metallurgy

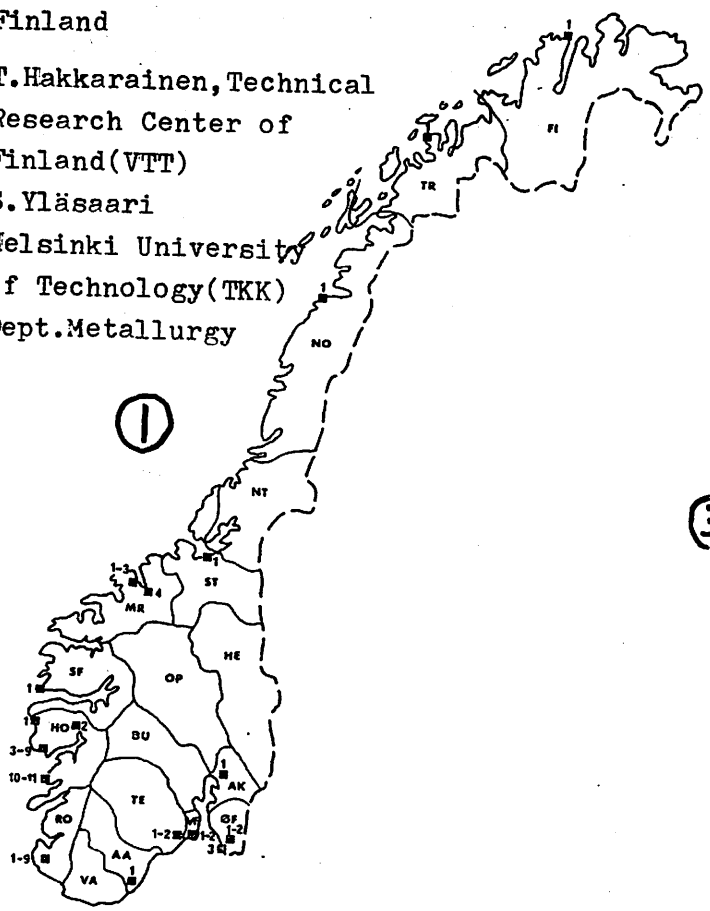

Figure 60.1. Corrosion test sites in Norway—numbered for each county (Table 60.3).

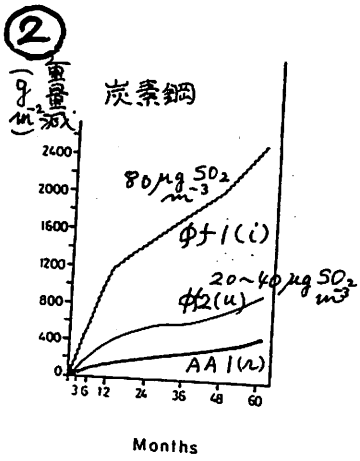

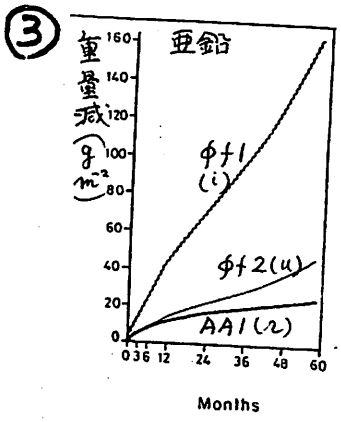

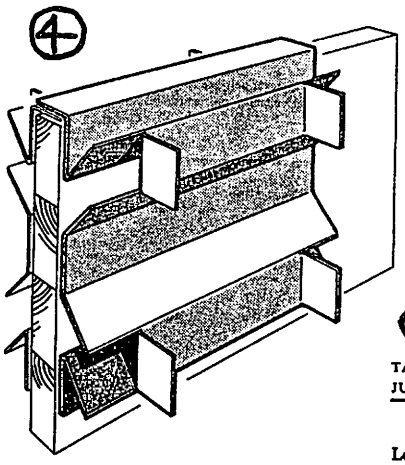

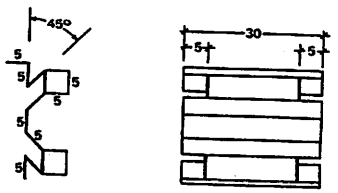

Figure 60.7. Test specimen configuration—coil-coated sheet. Dimensions in centimeters (5 cm = 2 in.).

Station	Carbon steel (series 1) ΔW (g/m²)	Carbon steel (series 1) Annual rate (μm/yr)	Weathering steel (series 4) ΔW (g/m²)	Weathering steel (series 4) Annual rate (μm/yr)	Relative corrosion rate: weathering steel / carbon steel
SF 1 Hyllestad	201	6.4	124	3.9	62%
Ho 2 Voss	151	4.8	94	3.0	62%
Ho 4 Bg. Tidende	390	12.4	114	3.6	29%
Ho 5 VERITAS	241	7.7	123	3.9	51%
Ho 9 Stend	212	6.7	131	4.2	62%
Ho 10 Stord 50	99	3.1	111	3.5	112%
Ho 3 Fredr.berg	243	7.7	136	4.3	56%
Ho 7 Minde	282	9.0	163	5.2	58%

TABLE 60.10 ATMOSPHERIC CORROSION OF VARIOUS METALS—ALL EXPOSURES STARTED IN JULY 1971. (WEIGHT LOSS IN g/m²)

Location	Duration 1 Year	2 Years	3 Years	4 Years	5 Years	6 Years	8 Years
A. Commercially pure copper							
Ho 10 Stord 50	9.6	17.9	–	21.0	–	–	–
Ho 7 Bergen-Minde	11.8	19.8	–	30.0	34.0	36.0	–
B. Silicon-killed steel							
Ho 5 Bergen-VERITAS	340	512	–	660	736	784	862
Ho 3 Bergen-Fredriksberg	271	403	–	567	622	688	802
C. Silicon-killed, hot-dip galvanized steel							
SF 1 Sogn	7.94	15.08	–	31.1	41.1	47.6	58.0
Ho 5 Bergen-VERITAS	12.98	24.44	–	56.5	65.4	75.6	87.7
Ho 9 Bergen-Stend	6.67	17.61	–	27.3	35.2	35.7	53.3

Norway and Sweden V.Kucera, J.Gullman, Swedish Corrosion Inst, Stockholm

S.Haagenrud, Norwegian Inst. for Air Research, Lillestrom, Norway

Material	Insulation thickness (μm)	Impressed voltage (mV)
Carbon steel, weathering steel	400	200
Zinc	300	100
Copper	200-300	100
Aluminum	100	100

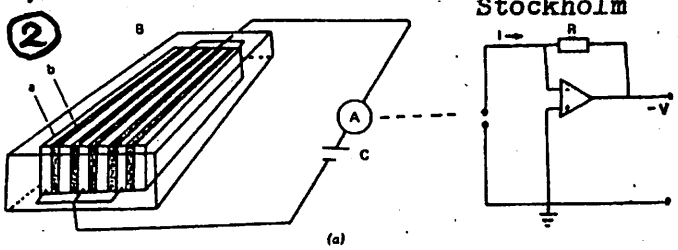

Figure 47.1a. General arrangement of electrochemical device for measurement of atmospheric corrosion: (A) is a zero resistance ammeter, the circuit of which is shown to the right; (B) is an electrolytic cell [(a) electrodes, (b) insulators]; (C) is a constant DC voltage source.

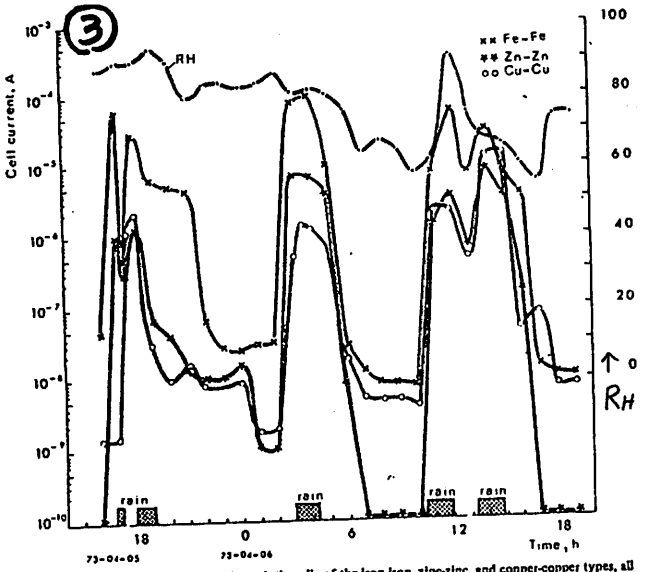

Figure 47.2. Cell current in electrolytic cells of the iron-iron, zinc-zinc, and copper-copper types, all with an imposed emf of 100 mV, and the relative humidity in Stockholm over the period of 5 April-7 April 1973 [1].

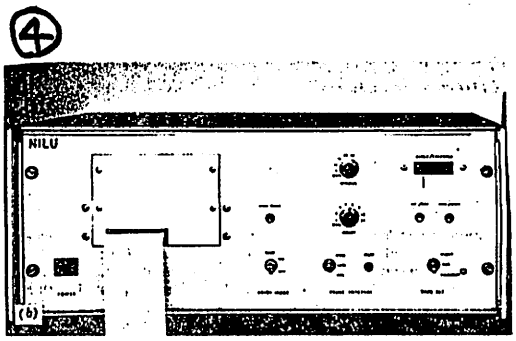

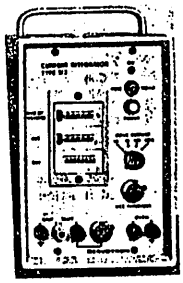

Figure 47.1b. Electronic integrator with automatic changeover between two current ranges and with registration of time-of-wetness (right) and automatic 12-channel printer for reading of integrated current and time-of-wetness (left).

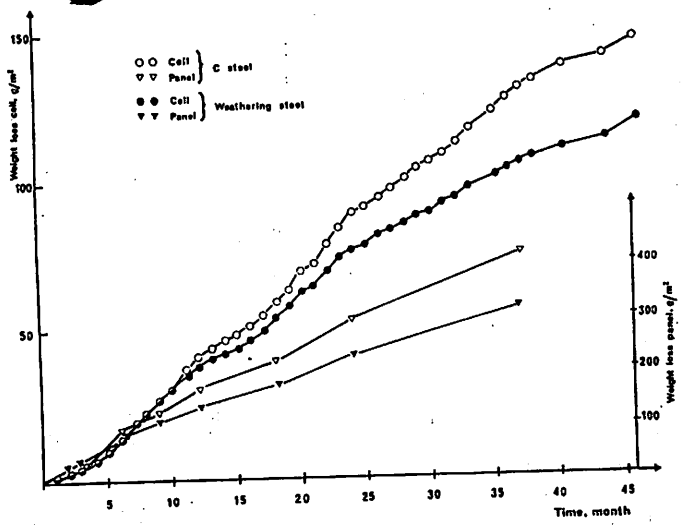

Figure 47.5. Integrated current from carbon steel and weathering steel cells converted to weight loss and weight loss of panels during outdoor exposure in Stockholm from June 1975 to April 1979.

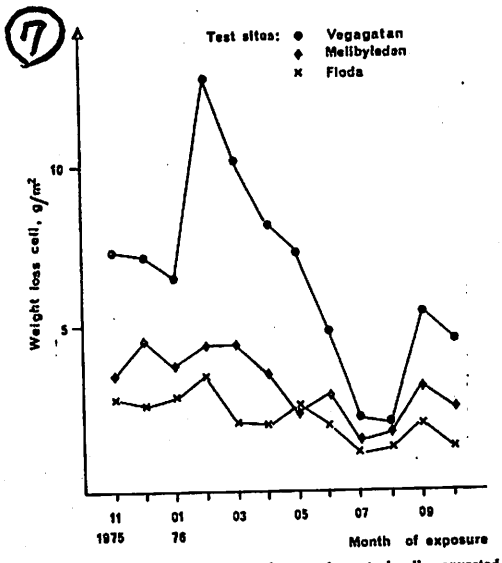

Figure 47.14. Integrated current from carbon steel cells converted to weight loss during different months.